Chemical Geology 466 (2017) 617–626

Contents lists available at ScienceDirect

Chemical Geology

journal homepage: www.elsevier.com/locate/chemgeo

Investigating arsenic speciation in the JEB Tailings Management Facility at McClean Lake, Saskatchewan using X-ray absorption spectroscopy

Peter E.R. Blanchard[a,*], Lisa L. Van Loon[a], Joel W. Reid[a], Jeffrey N. Cutler[a], John Rowson[b], Kebbi A. Hughes[b], Caitlin B. Brown[b], John J. Mahoney[c], Liying Xu[d], Matthew Bohan[d], George P. Demopoulos[d]

[a] Canadian Light Source, Saskatoon, SK S7N 2V3, Canada
[b] AREVA Resources Canada, Saskatoon, SK S7K 3X5, Canada
[c] Mahoney Geochemistry Consulting LLC, Lakewood, CO 80226, United States
[d] Department of Mining and Materials Engineering, McGill University, Montreal, QC H3A 0C5, Canada

ARTICLE INFO

Keywords:
Arsenic speciation
Mine tailings
Environmental geochemistry
X-ray absorption spectroscopy

ABSTRACT

AREVA Resources Canada operates the McClean Lake Operation (MLO), a uranium mine and processing facility located in northern Saskatchewan. Uranium-containing ores processed at the MLO contain high concentrations of arsenic that is oxidized to soluble arsenite and arsenate species when leaching and recovering uranium. To reduce the environmental impact of AREVA's mining operations, AREVA has developed a tailings preparation process designed to trap arsenic in a mineral form before the tailings are permanently deposited in the JEB Tailings Management Facility (TMF). Scorodite ($FeAsO_4{\cdot}2H_2O$) is predicted to be the primary arsenic species produced from the tailings preparation process. However, scorodite has never been observed in aged tailings samples. Confirming the presence of scorodite in the tailings is important in verifying that the tailings preparation process at the MLO can isolate high concentrations of arsenic from the environment in the form of stable minerals. Herein, X-ray Absorption Near-Edge Structure (XANES) spectroscopy was used to investigate arsenic speciation in a series of samples collected from the JEB TMF in 2013. Arsenic K-edge XANES analysis confirmed that most (86 wt%) of the arsenic content in the tailings samples consisted of iron-containing arsenates. Of these, crystalline scorodite was the most abundant arsenate species followed by poorly crystalline arsenates in the form of poorly crystalline ferric arsenate ($FeAsO_4{\cdot}xH_2O$) and arsenate adsorbed on ferrihydrite (AsO_4–FeOOH). Arsenite adsorbed on ferrihydrite (AsO_3–FeOOH), and gersdorffite (NiAsS) were also identified as minor arsenic species in the tailings samples. The abundance and distribution of scorodite in the TMF suggests that it is the major arsenic species produced in the tailings preparation process.

1. Introduction

AREVA Resources Canada Inc. (AREVA) is the principle owner of the McClean Lake Operation (MLO), a uranium mill in the Athabasca basin of northern Saskatchewan, Canada. The MLO commenced operation in 1999 with an anticipated long operating life, approximately five decades, with more than half a dozen uranium ore bodies scheduled to be processed over that duration. The most common uranium-containing mineral processed at the MLO is uraninite (UO_2). Uranium is extracted from the ore using a hydrometallurgical process involving hydrogen peroxide (H_2O_2), and sulfuric acid (H_2SO_4). The MLO process has been optimized for uranium recovery and high uranium leaching efficiencies of approximately 99% are achieved. However, uranium ore bodies in the Athabasca basin are typically comineralized with minerals containing arsenic. Gersdorffite (NiSAs), niccolite (NiAs), rammelsbergite ($NiAs_2$), and skutterudite ($NiAs_3$) are the principle arsenic bearing minerals in the ores processed at the MLO with concentrations ranging from ~300 μg/g to ~50,000 μg/g (Hoeve and Quirt, 1987; Reyx and Ruhjmann, 1993). Within the constraints of the uranium extraction process, 70–95% of the arsenic is leached from the ores as soluble arsenite ($[AsO_3]^{3-}$; As^{3+}) and arsenate ($[AsO_4]^{3-}$, As^{5+}) species in concentrations ranging from ~100 mg/L to ~10,000 mg/L. Following the extraction and recovery of uranium, the soluble arsenic species remain in an acidified waste solution known as the raffinate with small amounts of primary arsenic minerals remaining in the leach residue solids.

It is incumbent upon AREVA to ensure that the MLO incorporates robust processes for the protection of the environment from the harmful

* Corresponding author.
E-mail address: peter.blanchard@lightsource.ca (P.E.R. Blanchard).

http://dx.doi.org/10.1016/j.chemgeo.2017.07.014
Received 16 August 2016; Received in revised form 10 July 2017; Accepted 17 July 2017
Available online 22 July 2017

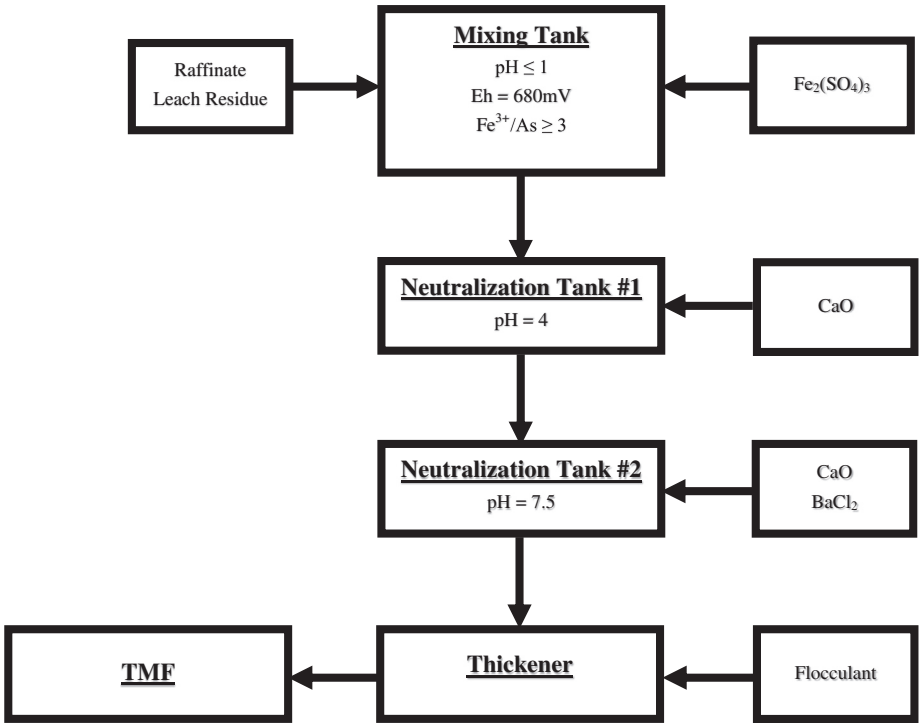

Fig. 1. Schematic of the tailings preparation process used at the McClean Lake Operation. The pH and Eh are controlled in the mixing tanks through the addition of sulfuric acid and hydrogen peroxide, respectively.

elements that co-mineralize with uranium, particularly arsenic. To this end, raffinate and leach residue undergo additional tailings preparation to prevent the release of soluble arsenic species. A flow diagram of the tailings preparation process is shown in Fig. 1. The raffinate and leach residue are first transferred to a mixing tank where the pH and Eh are controlled to approximately 1 and + 680 mV, respectively. Ferric sulfate ($Fe_2(SO_4)_3$) is continuously added to maintain a Fe^{3+}/As molar ratio of at least 3. The pH is first raised to 4 and finally to 7.5 through the controlled addition of lime (CaO) in subsequent reactor tanks. Each reactor tank provides a retention time of 90 min. The treated and neutralized tailings are then fed to a thickener to create "thickened" tailings for permanent disposal in the JEB Tailings Management Facility (TMF). The solid component of the tailings slurry pumped to the TMF consists of leach residue minerals (i.e. primary mineralization) and precipitated phases from the neutralized raffinate solution (i.e. secondary mineralization) in approximately equal abundance. The leach residue component consists of mostly unreacted quartz (SiO_2) and various clay minerals. Except for gypsum ($CaSO_4{\cdot}2H_2O$), the secondary mineralization exists in poorly crystalline and/or amorphous forms.

The tailings preparation process at the MLO is unique in the mining industry in two ways: 1) the addition of ferric sulfate to adjust the Fe^{3+}/As ratio and 2) a near-neutral terminal discharge pH. Tailings produced by gold and uranium mining operations typically use iron in the ore to control the release of arsenic and are discharged at a much higher terminal pH (10 − 12) (Essilfie-Dughan et al., 2013; Foster et al., 1998; Moldovan et al., 2003; Moldovan and Hendry, 2005; Paktunc et al., 1998; Paktunc et al., 2003, 2004; Pichler et al., 2001; Robertson et al., 2014; Roussel et al., 2000; Shaw et al., 2011). Under these conditions, arsenic concentrations are controlled by adsorption of arsenate onto ferrihydrite (AsO_4–FeOOH). However, the stability of arsenic is dependent upon the availability of sufficient iron in the ore to adsorb arsenic. At the MLO, some of the ore bodies to be processed contain significantly more arsenic than iron and cannot rely on adsorption to control the release of arsenic. The tailings preparation process was designed to respond to the wide range of arsenic concentrations found in the ores to be processed at the MLO through the controlled addition of Fe^{3+}.

Early studies conducted to support the operating licence of the MLO predicted that arsenic in the raffinate solution would precipitate primarily as a poorly crystalline form of scorodite. ($FeAsO_4{\cdot}2H_2O$), with secondary arsenate adsorption onto ferrihydrite at a near neutral pH (Langmuir et al., 1999a,b). Sequestering arsenic in uranium mine tailings via mineralization rather than adsorption is unique to the MLO. The mineralogical endpoint with respect to arsenic was also predicted to be consistent for all of the ores scheduled to be processed by the MLO if the Fe^{3+}/As ratio was > 3. Neutralization studies were later performed using actual raffinate solution produced at the MLO to determine how arsenic reacts with iron as a function of pH. It was found that arsenic and iron coprecipitate in a near 1:1 ratio as poorly crystalline ferric arsenate ($FeAsO_4{\cdot}xH_2O$) up to a pH of 3.23 (Langmuir et al., 2006; Mahoney et al., 2007). The excess iron precipitating as ferrihydrite as the pH is increased to 7.32. Extended X-ray Absorption Fine Structure (EXAFS) analysis of neutralized raffinate solids later indicated that the poorly crystalline ferric arsenate species that forms at low pH has local structure similar to scorodite (Chen et al., 2009). This was the first concrete mineralogical evidence of the occurrence of a poorly crystalline scorodite phase in neutralized mine raffinate solids. The poorly crystalline form of scorodite was found to be stable up to a pH of 7.02 where a small amount of scorodite was found to dissolve and likely adsorbed on ferrihydrite (Chen et al., 2009). However, a significant amount of poorly crystalline scorodite remains at a near-neutral pH.

Although scorodite was found to precipitate in neutralized raffinate solutions under various laboratory conditions, scorodite has yet to be identified in actual tailings deposited in the TMF. Confirming the presence of scorodite in the tailings is important in verifying that the tailings preparation process at the MLO can isolate high concentrations of arsenic from the environment in the form of stable minerals. To this end, X-ray Absorption Near-Edge Structure (XANES) spectroscopy was used to investigate the arsenic speciation in the TMF. XANES analysis identified various arsenic species of different oxidation states. Scorodite was confirmed to be the most abundant arsenic species in the TMF. The distribution of the various arsenic species is discussed.

Table 1
Reactions used in the diffuse layer for the adsorption of arsenate and arsenite onto ferrihydrite.
Equilibrium constants were obtained from Dzombak and Morel (1990) and Gustafsson and Bhattacharya (2007).

Reactions	LogK	
	Dzombak et al.	Gustafsson et al.
Arsenate		
FeOOH-OH + $[AsO_4]^{-3}$ + $3H^+$ → FeOOH-H_2AsO_4 + H_2O	29.31	30.98
FeOOH-OH + $[AsO_4]^{-3}$ + $2H^+$ → FeOOH-$[HAsO_4]^-$ + H_2O	23.51	25.84
FeOOH-OH + $[AsO_4]^{-3}$ + H^+ → [FeOOH-$AsO_4]^{-2}$ + H_2O	N/A	19.5
FeOOH-OH + $[AsO_4]^{-3}$ → [FeOOH-$OHAsO_4]^{-3}$	10.58	11.92
Arsenite		
FeOOH-OH + H_3AsO_3 → FeOOH-H_2AsO_3 + H_2O	5.41	5.27
FeOOH-OH + H_3AsO_3 → FeOOH-$[HAsO_3]^-$ + H^+ + H_2O	2.91	N/A

2. Experimental

2.1. Tailings samples selection and characterization

Fifty tailings samples were collected in 2013 for the Tailings Optimization and Validation Program (TOVP) by the AREVA Resources Canada Safety, Health, Environmental, and Quality (SHEQ) Department. Tailings samples were collected from three bore hole locations: TMF13-01 (located at the centre of the TMF), TMF13-02 (located an intermediate distance from the centre), and TMF13-06 (located at the periphery of the TMF). The exact locations of the bore holes are highlighted on the map shown in Fig. A1 in the Appendix. The tailings are placed in the TMF using a centrally located floating barge and tremie piping system. While the design minimizes particle size segregation at the point of placement, it does not eliminate it. The central bore hole consists of a coarser particle size distribution than the peripheral bore hole. This results in larger grains of primary mineralization collecting near the centre of the TMF and a greater abundance of finer particles of secondary mineralization drifting to the periphery of the TMF. Samples were collected from each bore hole using a thin walled sampler that was lowered through a sealed casing and pushed into the tailings to collect intact samples. A commercially available Gregory type piston sampler uses hydraulic pressure to extrude a standard stainless steel Shelby tube into the tailings to collect a 1 m sample in 3 m intervals. Upon retrieval of each tailings sample, the temperature was measured and the Shelby tube ends were capped and sealed. Samples were stored vertically in an ice water bath maintained at ~278 K to minimize exposure of the sample to oxygen. Tailings at the end of the Shelby tube, which was exposed to air, were discarded to ensure that fresh samples were analyzed. Pore water was extracted using a hydraulic press and collected in a 60 mL syringe. The tailings solids were nitrogen-purged, vacuum-sealed, and stored in a freezer to limit the effects of oxidation. Samples were transported to the CLS at ~193 K and stored at this temperature to prevent the tailings solids from undergoing chemical reactions after they had been extracted from the TMF.

The total arsenic and iron concentration of the tailings solids was quantified by inductively coupled plasma-mass spectrometry (ICP-MS) analysis performed at Saskatchewan Research Council Environmental Analytical Laboratories. The concentration of arsenic in the tailings solids varied from 62 to 16,000 μg/g, with higher concentrations found in samples collected from the peripheral bore hole. Results of this analysis can be found in the Appendix.

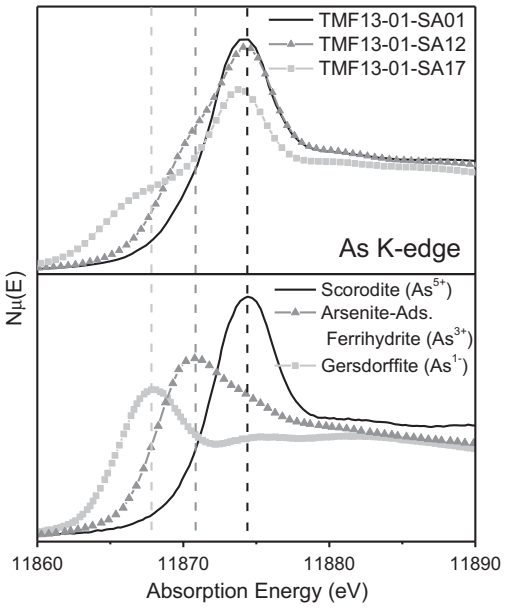

Fig. 2. The arsenic K-edge XANES spectra of a) selected tailings samples and b) arsenic standards highlighting spectral features that corresponds to As^{5+} (11,874.3 eV; black dash line), As^{3+} (11,870.8 eV; grey dash line), and As^{1-} (11,868.1 eV; light grey dash line).

2.2. Preparation and characterization of arsenic standards

Arsenic mineral standards were purchased, obtained as a mineral sample, or synthesized. Arsenolite (As_2O_3; 99.9% purity) and calcium arsenate ($Ca_3(AsO_4)_2$; 99.9% purity) were purchased from Alfa-Aesar. Gersdorffite (NiAsS) was obtained from the Royal Ontario Museum. Niccolite (NiAs) and rammelsbergite ($NiAs_2$) were obtained from the Cameco Corporation. Arsenopyrite (FeAsS) was purchased as a reference material. Synthesized standards included arsenate adsorbed on ferrihydrite (AsO_4–FeOOH), arsenite adsorbed on ferrihydrite (AsO_3–FeOOH), arsenite solution ($[AsO_3]^{3-}_{(aq)}$), poorly crystalline ferric arsenate ($FeAsO_4{\cdot}xH_2O$), scorodite ($FeAsO_4{\cdot}2H_2O$), annabergite ($Ni_3(AsO_4)_2{\cdot}8H_2O$), yukonite ($Ca_7Fe_{12}(AsO_4)_{10}(OH)_{20}{\cdot}15H_2O$), and tooeleite ($Fe_6(AsO_3)_4SO_4(OH)_4{\cdot}4H_2O$). Synthesis details are found in the Appendix.

2.3. Synchrotron X-ray Diffraction

Synchrotron X-ray Diffraction (S-XRD) of select tailings samples and reference materials were collected at the Canadian Macromolecular Crystallography Facility (CMCF) (beamline 08ID-1) at the Canadian Light Source (CLS) (Fodje et al., 2014). Patterns were collected at room temperature over an angular range of $2^o \leq 2\theta \leq 39^o$ using a X-ray wavelength of 0.6888 Å. Each finely ground sample was placed in a 0.5 mm diameter Kapton capillary that was rotated during data collection. Two-dimensional (2D) patterns were obtained using a Rayonix MX300HE detector with an active area of 300 mm × 300 mm.

The 2D patterns were calibrated and integrated using the GSAS II software package (Toby and Von Dreele, 2013). The sample-detector distance, detector centering, and detector tilt were calibrated for all patterns using a lanthanum hexaboride standard reference material (NIST SRM660a LaB_6). A background subtraction was applied using a pattern collected from an empty Kapton capillary. Phase identification was performed using the Powder Diffraction File (PDF-4 + 2013) software package (Powder Diffraction File, 2013). The S-XRD patterns of the reference materials and select tailings samples are shown in the Appendix (see Figs. A2–A8).

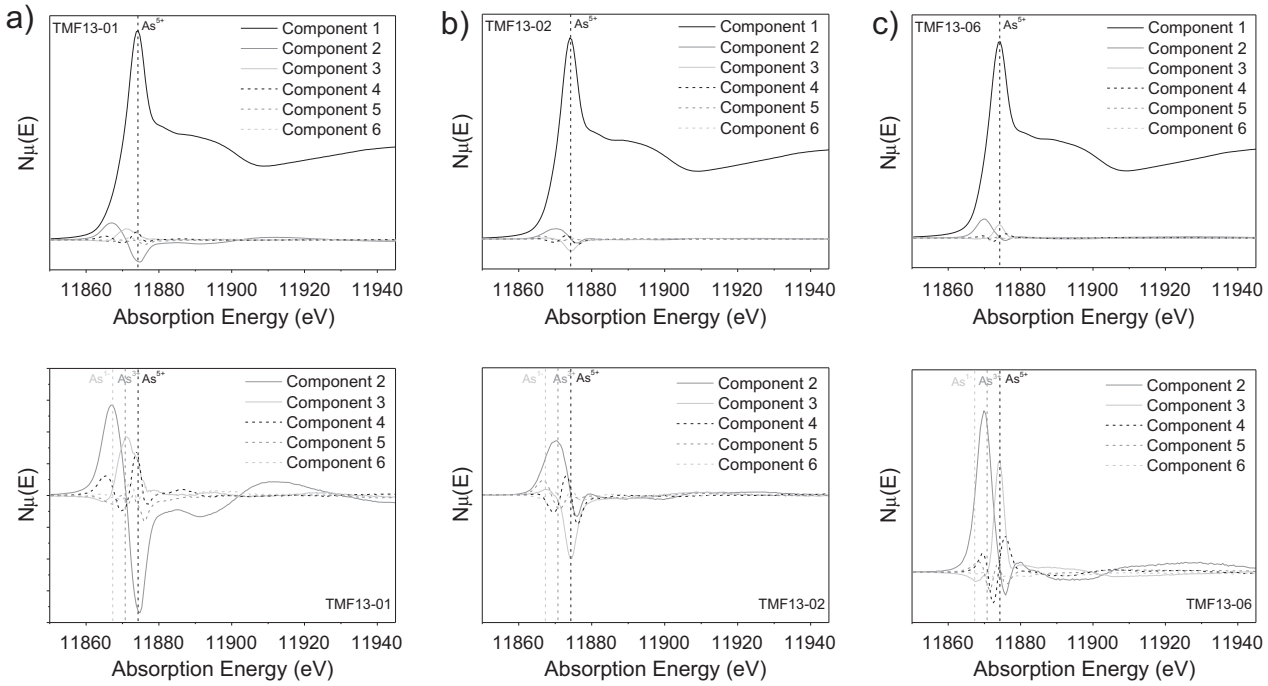

Fig. 3. The principle components calculated in the PCA of tailings samples from bore holes a) TMF13-01, b) TMF13-02, and c) TMF13-06. Component 1 (top) has the strongest intensity, accounting for > 98% of the variances. The dashed line corresponds to the expected first peak position for an As^{5+} oxidation state. Components 2–6 (bottom) have peak maxima and minima at energy positions expected for As^{5+}, As^{3+}, and As^{1-} oxidation states.

2.4. Arsenic K-edge XANES spectroscopy

The arsenic K-edge XANES measurements of both the tailings samples and reference materials were performed on the Hard X-ray MicroAnalysis (HXMA) superconducting wiggler beamline (06ID-1) at the CLS (Jiang et al., 2007). Clumps of sample were broken up and mounted in rectangular metal holders that were sealed using a single layer of Kapton tape. Images of two mounted samples are shown in the Appendix (Fig. A9). Standards were diluted with boron nitride (BN) and mounted into Teflon sample holders sealed with a single layer of Kapton tape. For measurements, samples were positioned in front of the X-ray beam at a 45° angle and cooled to ~50 K using a closed-cycle cryostat to prevent beam-induced reduction. Spectra were collected from − 200 eV to + 320 eV relative to the arsenic K-edge absorption edge (11,867 eV) with a step size of 0.3 eV near the edge. The energy range was selected using a silicon (111) crystal monochromator, which provided a monochromatic flux of $\sim 10^{12}$ photons/s with a resolution of 1 eV at 10 keV. All spectra were measured in partial fluorescence yield (PFY) mode using a Canberra Discrete Array 32 element germanium detector (Canberra Industries Inc.) and calibrated against a gold metal foil standard (EXAFS Materials), with the maximum of the first derivative of the gold L_3-edge set to 11,919 eV (Ravel and Newville, 2005). Multiple scans were collected for each spectrum. It was concluded that the samples did not undergo any X-ray beam-induced reduction as there were no changes in the spectra between successive scans. All XANES spectra were analyzed using the Athena software program version 0.9.20 (Ravel and Newville, 2005). Principal Component Analysis (PCA) was performed to identify the number of arsenic components in the spectra followed by Linear Combination Fitting (LCF) to identify the arsenic species in the tailings samples. The energy range used in the PCA and LCF analyses was − 20 eV to + 80 eV relative to the arsenic K-edge absorption edge energy.

2.5. Thermodynamic data

Eh-pH diagrams of the Ni-Fe-As-Ca-S-O_2-H_2O system were prepared to provide thermodynamic context to the arsenic species distribution in the JEB TMF. The model was based on the several previously reported reaction constants (Mahoney et al., 2007). The concentrations used to construct the Eh-pH diagram were obtained from the average concentrations found in the tailings pore water (AREVA Resources Canada Ltd., 2015). Primary arsenic mineralization is represented in the Eh-pH diagram as niccolite.

A series of geochemical models were prepared to illustrate the extent of arsenate and arsenite surface complexation that can occur within the pH range of the TMF. The models were based on the original diffuse layer model prepared by Dzombak, and Morel that provided a set of arsenate and arsenite complexation constants onto the ferrihydrite surface (Dzombak and Morel, 1990). Gustafsson and Bhattacharya updated these reactions using various data sources from more recent literature (Gustafsson and Bhattacharya, 2007). In general, they increased the arsenate surface complexation constants by one to two orders of magnitude and decreased the arsenite surface complexation constant. Gustafsson and Bhattacharya also added additional arsenate and arsenite complexation reactions to the models that are dominate at higher pH (Gustafsson and Bhattacharya, 2007). The reactions and surface complexation constants used in the diffuse layer model are listed in Table 1. To better show the slight difference between the arsenite and arsenate surface complexes, the models were run at relatively low sorption capacities. The two valences of arsenite and arsenate were defined in separate solutions and the surface complexation reactions used the same surface but were modelled independently. A weak site concentration of 2.5×10^{-4} mol/L was used to define the ferrihydrite surface. The site concentration is based upon 0.122 g/L of ferrihydrite at a proportion of 0.2 weak sites per mole of ferrihydrite precipitated. The surface area was assumed to be 600 m^2/g. Strong sites were also included at 6.25×10^{-6} mol/L, but these sites do not complex with anions. The initial concentration for either arsenite or arsenate was set at 10 mg/L.

An Eh-pH diagram of arsenate and arsenite complexation on a hybrid ferrihydrite goethite surface was also prepared to show the stability of various adsorbed species under a wide range of Eh and pH values. The Eh-pH diagrams used the same surface complexation constants as defined in Table 1, but the surface site density was reduced from

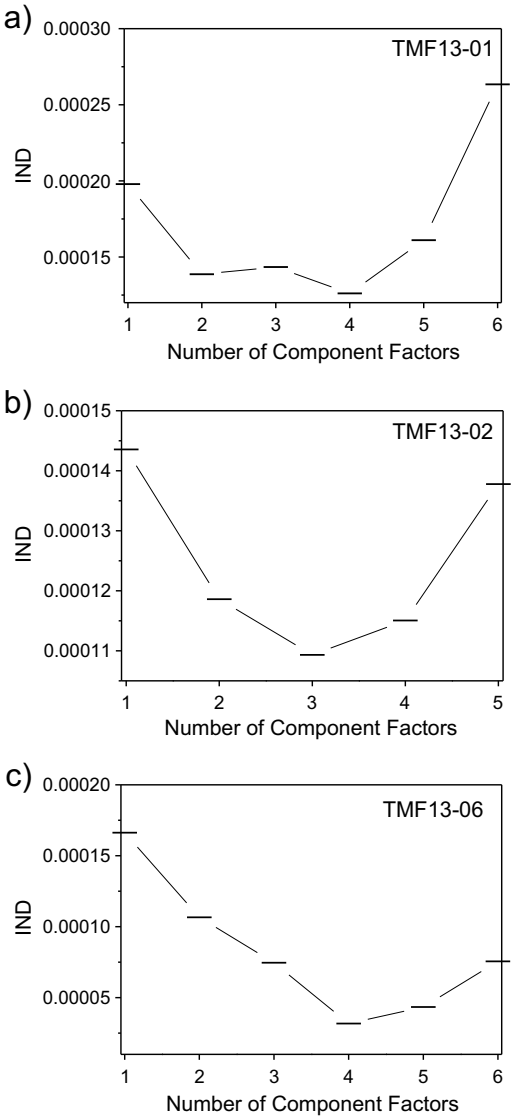

Fig. 4. The IND values as a function of the number of component factors for a) TMF13-01, b) TMF13-02, and c) TMF13-06 sample sets. The IND values are minimized at three or four factors, suggesting that each spectrum contains up to four components.

0.2 mol of sites per mole of iron precipitate to 0.1 mol of weak sites, and the surface area was reduced to 60 m^2/g. This composite surface is an approximation of ferrihydrite converting to goethite. The goethite concentration was set at 0.05 mol/L. All modelling calculations were run in PHREEQC software program (Kinniburgh and Cooper, 2011). All Eh-pH diagrams were prepared using the PhreePlot software program (Parkhurst and Appelo, 2013).

3. Results

3.1. Arsenic K-edge XANES spectroscopy

The arsenic K-edge XANES spectra of the tailings samples and arsenic standards were collected and analyzed. Representative spectra of the tailings samples are shown in Fig. 2. The arsenic K-edge XANES spectra for all tailings samples and standards are shown in the Appendix (Figs. A10–A13). The absorption edge energy and lineshape of the arsenic K-edge is sensitive to the oxidation state and chemical environment of the absorbing arsenic atoms. The arsenic K-edge XANES spectra consist of two features: The first peak (~11,865–11,875 eV) corresponds to a dipole-allowed transition of a 1s electron into unoccupied 4p states. The absorption energy of this feature is sensitive to the oxidation state of arsenic, shifting to higher energy with increasing oxidation state (Wang et al., 2013; Lin et al., 2014). The increase in oxidation state decreases the screening of the core electron, creating a more tightly bounded final state (Newville, 2004). As a result, higher energies are required to excite the 1s electron into the unoccupied 4p states. Three distinct energy positions for this peak are observed in the arsenic K-edge XANES spectra of the tailings samples (Fig. 2). The position of this peak indicates the presence of As^{5+}, As^{3+}, or As^{1-} oxidation states.

A broad feature is found at higher absorption energy (~11,875–11,895 eV). This feature consists of significant contributions from Multiple Scattering Resonances (MSR), which is a low-energy EXAFS phenomenon that is dependent on the local structure of the absorbing atom (Rehr and Albers, 2000). The energy and intensity of this feature is dependent on crystal structure and crystallinity (Kutzler et al., 1980). The lineshape of the MSR feature of the tailings samples is similar to that of the iron-containing arsenate standards (see Fig. A13 in the Appendix), suggesting that iron-containing arsenates are present in the tailings samples.

3.1.1. Principle component analysis (PCA)

Information beyond oxidation states and basic information on local chemical environment can be obtained using advanced quantitative XANES analyses. PCA was first used to determine the number of arsenic phases present in the tailings samples and to serve as an overall guide for the LCF analysis. In the PCA calculation, a series of spectra are decomposed into components (eigenvectors) and weights (eigenvalues) that represent the variation in the spectra. The assumption in applying PCA is that XANES spectra are linear combinations of the individual arsenic components in the sample. The minimum number of components required to explain the variation in a group of spectra is the number of major chemical species contributing to the spectra (Malinowski, 2002). The minimum number of components can be tested against an indicator function known as an IND. The number of components that give the minimum IND value corresponds to the number of chemical species present in the spectra (Fernández-García et al., 1995). PCA analysis was performed on samples from three bore holes (TMF13-01, TMF13-02, TMF13-06). Differences in the lineshapes of the calculated components suggest variations in the chemical composition within each bore hole.

Results of the PCA analysis are shown in Fig. 3. The number of components calculated in PCA is related to the different arsenic-containing species in the tailings samples. In all three bore hole sets, the first calculated component has the largest amplitude and accounts for over 98% of the total variance in the spectra. The first component is an average of all the spectra and describes the overall edge jump (Beauchemin et al., 2002). The amplitudes are significantly smaller for the other components as they account for the small differences between spectra. The lineshape of the first component calculated in each PCA is similar to the As^{5+} standards, suggesting that the major component is an As^{5+} species. The distinguishing features in components 2–6 (i.e. maxima and minima) corresponds to the peak energies of various arsenic oxidation states, suggesting variations in the composition of minor arsenic species. For example, components 2–4 generally have relatively large peak minima and maxima at energies where significant spectral features are observed for As^{5+}, As^{3+} and As^{1-} species. The IND values approached a minimum between two and four components (Fig. 4), indicating that each tailings sample contain between two and four arsenic-containing species.

3.1.2. Linear Combination Fitting (LCF) analysis

LCF analysis was used to identify the arsenic-containing species present in the tailings samples. In the LCF analysis, the spectra of the tailings samples were fitted to a linear combination of weighted standard spectra. The standard spectra used in the LCF are shown in Fig.

Table 2
Summary of the LCF analysis of the tailings samples. The concentration (μg/g) of each arsenic mineral species was calculated from the total concentration of arsenic in the tailings samples (Table A1, Appendix).

Sample	PC ferric arsenate		Scorodite		Arsenite ads. ferrihydrite		Gersdorffite	
	at.%	μg/g	at.%	μg/g	at.%	μg/g	at.%	μg/g
TMF13-01-SA01	16 ± 7	1200 ± 600	70 ± 5	6000 ± 1000	14 ± 8	500 ± 200		
TMF13-01-SA03			75 ± 6	2900 ± 500	25 ± 8	450 ± 90		
TMF13-01-SA04	32 ± 7	300 ± 70	48 ± 5	520 ± 70	20 ± 6	100 ± 40		
TMF13-01-SA05			80 ± 4	3200 ± 500	20 ± 7	400 ± 300		
TMF13-01-SA06	66 ± 7	370 ± 50			34 ± 10	100 ± 40		
TMF13-01-SA08	68 ± 6	270 ± 30			32 ± 4	70 ± 20		
TMF13-01-SA09	41 ± 8	280 ± 60	43 ± 5	350 ± 50	16 ± 8	60 ± 40		
TMF13-01-SA10	50 ± 6	150 ± 20			50 ± 9	80 ± 20		
TMF13-01-SA11	50 ± 8	150 ± 20			50 ± 9	80 ± 20		
TMF13-01-SA12	56 ± 10	210 ± 40			44 ± 15	90 ± 30		
TMF13-01-SA14	76 ± 6	100 ± 10			24 ± 9	20 ± 10		
TMF13-01-SA15	86 ± 4	230 ± 20			14 ± 4	20 ± 10		
TMF13-01-SA16	57 ± 6	120 ± 20			43 ± 9	50 ± 20		
TMF13-01-SA17	40 ± 5	80 ± 10					60 ± 3[a]	120 ± 10
TMF13-01-SA19	58 ± 2	180 ± 20			42 ± 4	140 ± 10		
TMF13-01-SA20	65 ± 3	220 ± 20			35 ± 3	60 ± 10		
TMF13-01-SA21	59 ± 6	200 ± 30			31 ± 3	60 ± 10	11 ± 8	30 ± 20
TMF13-01-SA22	42 ± 3	580 ± 90			47 ± 4	360 ± 70	11 ± 8	130 ± 90
TMF13-01-SA23			47 ± 2	600 ± 100	24 ± 2	150 ± 30	29 ± 3	280 ± 50
TMF13-01-SA24	47 ± 4	35 ± 5	10 ± 4	9 ± 3	43 ± 6	18 ± 2		
TMF13-01-SA25	79 ± 5	6000 ± 1000			21 ± 8	900 ± 300		
TMF13-02-SA01			73 ± 5	8000 ± 1000	27 ± 5	1500 ± 500		
TMF13-02-SA02			65 ± 3	1100 ± 200	15 ± 3	120 ± 50	20 ± 5	300 ± 200
TMF13-02-SA04	61 ± 5	500 ± 90			39 ± 4	180 ± 50		
TMF13-02-SA05	25 ± 6	70 ± 20	60 ± 5	190 ± 30			15 ± 6	30 ± 20
TMF13-02-SA06	71 ± 8	580 ± 70			29 ± 6	130 ± 20		
TMF13-02-SA07	23 ± 5	200 ± 50	52 ± 5	510 ± 70	24 ± 8	110 ± 30		
TMF13-02-SA09	47 ± 3	260 ± 30	42 ± 4	280 ± 40	10 ± 5	30 ± 10		
TMF13-02-SA10	69 ± 7	80 ± 10			31 ± 10	20 ± 6		
TMF13-02-SA11	78 ± 5	68 ± 7			22 ± 7	10 ± 5		
TMF13-02-SA12	45 ± 9	140 ± 20			55 ± 11	90 ± 20		
TMF13-02-SA14	54 ± 11	150 ± 30			46 ± 15	70 ± 20		
TMF13-02-SA15	61 ± 5	210 ± 30			39 ± 5	70 ± 20		
TMF13-02-SA16	43 ± 5	230 ± 30			44 ± 2	130 ± 20	12 ± 8	50 ± 50
TMF13-02-SA17	37 ± 4	200 ± 40	21 ± 4	140 ± 20	42 ± 3	130 ± 20		
TMF13-02-SA19	54 ± 6	900 ± 200			46 ± 7	400 ± 100		
TMF13-02-SA20	44 ± 7	500 ± 80			56 ± 4	350 ± 50		
TMF13-02-SA21			86 ± 2	4400 ± 700	14 ± 2	300 ± 100		
TMF13-06-SA01			69 ± 12	13,000 ± 3000	31 ± 16	3000 ± 1000		
TMF13-06-SA03	18 ± 3	1800 ± 400	63 ± 4	7000 ± 1000	19 ± 5	1000 ± 500		
TMF13-06-SA04			88 ± 3	10,000 ± 2000	12 ± 4	600 ± 200		
TMF13-06-SA06	12 ± 3	1200 ± 300	88 ± 2	10,000 ± 1000				
TMF13-06-SA07	38 ± 5	1000 ± 200	27 ± 4	900 ± 200	33 ± 6	500 ± 100		
TMF13-06-SA09	21 ± 4	1500 ± 400	69 ± 3	6000 ± 900	10 ± 4	400 ± 200		
TMF13-06-SA11	21 ± 4	2200 ± 500	53 ± 5	7000 ± 1000	26 ± 7	1500 ± 400		
TMF13-06-SA12	67 ± 2	1100 ± 200			33 ± 4	570 ± 90		
TMF13-06-SA13	45 ± 3	400 ± 40			55 ± 5	270 ± 40		
TMF13-06-SA14	37 ± 4	320 ± 40	13 ± 4	100 ± 30	51 ± 7	240 ± 50		
TMF13-06-SA15	49 ± 5	900 ± 200			51 ± 6	500 ± 100		
TMF13-06-SA16	36 ± 6	600 ± 100	41 ± 5	800 ± 100	23 ± 9	200 ± 100		

[a] Spectrum was fitted using rammelsbergite rather than gersdorffite.

A13 in the Appendix. Several different combinations of standards were tested for each tailings spectrum and the total number of standards used in the LCF was restricted to four or less based on the results of the PCA. The coefficients calculated in the LCF, which correspond to the concentration of each arsenic species relative to the total concentration of arsenic in the tailings, was allowed to vary between zero and one with the total sum of the coefficients equal to one. Best fits were determined by calculating the goodness-of-fit parameters (R-value and χ^2). Generally, the fit with the smallest R-value and χ^2 value was considered the best. Decreasing the fitting range from 11,850–11,970 eV to 11,860–11,880 eV had no effect on the calculated concentrations, indicating that there are sufficient details in the first peak to distinguish between the different arsenic species in the tailings samples. An energy shift was not applied as the standards were calibrated to the same reference (i.e. Gold foil) as the tailings samples. The detection limit of the LCF analysis was assumed to be 10 at.% based on previous studies (Foster and Kim, 2014).

Results of the LCF analysis are tabulated in Table 2 and selected fitted arsenic K-edge XANES spectra from each bore hole are shown in Fig. 5. All fitted arsenic K-edge XANES spectra can be found in the Appendix (see Figs. A14–A60 in the Appendix). Good fits for most samples were obtained using scorodite, a poorly crystalline iron-containing arsenate, arsenite adsorbed on ferrihydrite, and gersdorffite. A better fit was obtained for the arsenic K-edge XANES spectrum of tailings sample TMF13-01-SA17 with rammelsbergite rather than gersdorffite (Fig. A27 in the Appendix). Decreasing the fitting range from 11,850–11,950 eV to 11,860–11,880 eV (i.e. the near-edge region) had little effect on the calculated concentrations, indicating that there are sufficient details in the near-edge region to distinguish between the different arsenic standards.

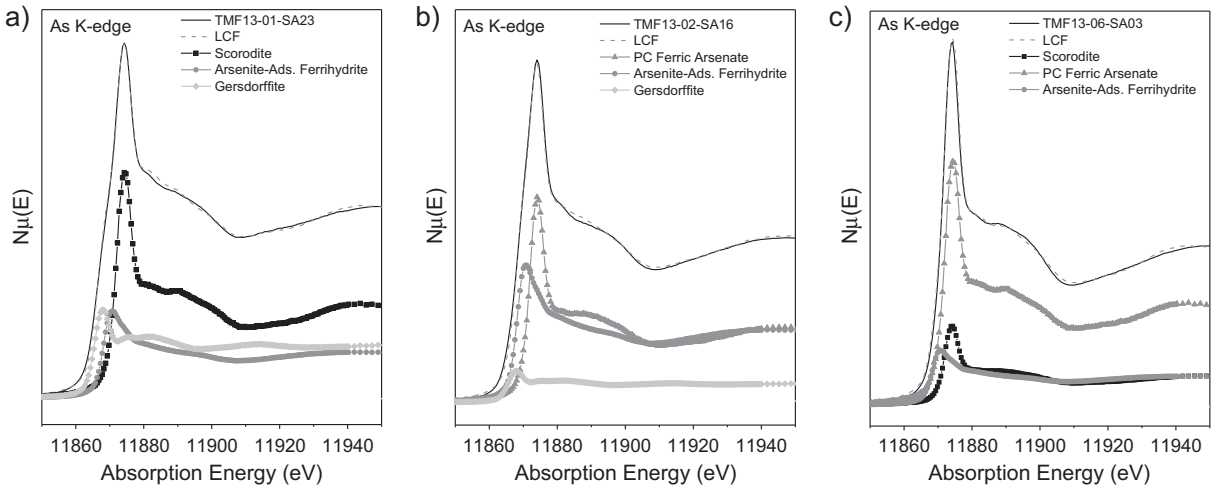

Fig. 5. The fitted arsenic K-edge XANES spectra of a) TMF13-01-SA23, b) TMF13-02-SA16, and c) TMF13-06-SA03. The weighted spectra of scorodite, poorly crystalline (PC) ferric arsenate, arsenite-adsorbed ferrihydrite, and gersdorffite are. Note that equally good fits were obtained when fitting the spectra to arsenate adsorbed on ferrihydrite rather than poorly crystalline ferric arsenate.

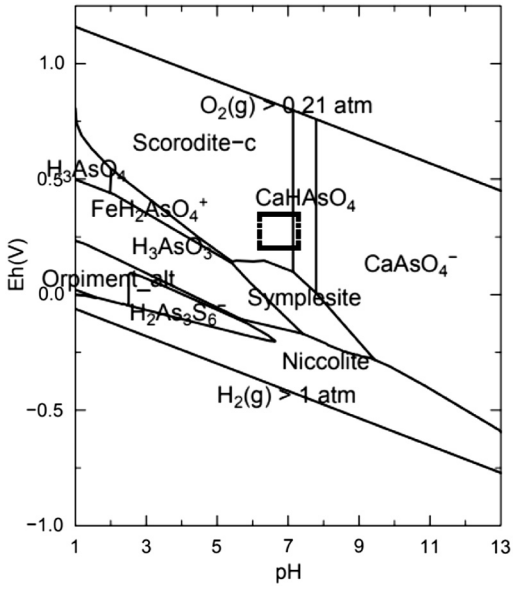

Fig. 6. Eh-pH diagram for the Ni-Fe-As-Ca-S-O_2-H_2O system at 25 °C showing the dominant dissolved and solid arsenic phases based on the pore water concentrations from the TMF ([Ni] = 10.0 mg/L; [As] = 5.0 mg/L; [Ca] = 400 mg/L; [Fe] = 500 mg/L; [SO_4^{2-}] = 2000 mg/L; [Mg] = 100 mg/L). The Eh and pH range found within the TMF are outlined by the black box which falls within the scorodite stability field.

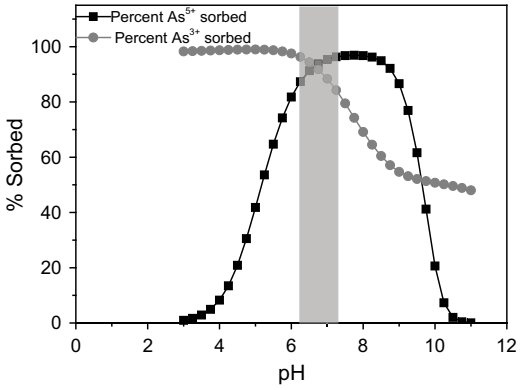

Fig. 7. Extent of arsenite and arsenate surface complexation plotted as a function of pH. The shaded region corresponds to the pH range of the TMF.

3.2. Thermodynamic data

An Eh-pH diagram showing the stability field for various dissolved and solid phases in a Ni-Fe-As-Ca-S-O_2-H_2O system is shown Fig. 6. The Ni-Fe-As-Ca-S-O_2-H_2O system is a close approximation to the conditions found in the TMF. Iron-containing arsenates are predominately stable under acidic (pH < 7), oxic conditions. In contrast, calcium-containing arsenates are most stable under basic (pH > 7.5), oxic conditions. Primary arsenic mineralization is mostly stable under anoxic conditions.

A series of PHREEQC calculations were also performed to determine the stability that arsenite and arsenate adsorbed species at various pH values. These calculations were performed assuming arsenite and arsenate adsorbs to ferrihydrite. The extent of arsenate and arsenite adsorption, calculated using the diffuse layer models described by Gustafsson and Bhattacharya, were plotted as functions of pH (see Fig. 7) (Gustafsson and Bhattacharya, 2007). Arsenite adsorption approaches a maximum in a pH range of 6–8. Arsenate adsorption, as a comparison, generally decreases with rising pH. Similar results were obtained when using the model described Dzombak, and Morel (see Fig. A61 in the Appendix) (Dzombak and Morel, 1990).

The Eh-pH diagram shown in Fig. 8a shows the stability of various soluble arsenic species in an As-O_2-H_2O system (i.e. aqueous solution). Soluble arsenous acid (H_3AsO_3) has a larger stability field than arsenic acid (H_3AsO_4) and deprotonates at relatively high pH of 9.2. For arsenic acid, the first deprotonation reaction happens around a pH of 2.24 and a second deprotonation reaction occurs at a pH of 6. The Eh-pH diagram shown in Fig. 8b shows the distribution of arsenate and arsenite adsorbed species, assuming adsorption to a ferrihydrite-goethite hybrid surface. Some of the reduced arsenic solids have been suppressed to better illustrate the distribution of the arsenite surface complexes. Two arsenite adsorbed species (H_3AsO_3—FeOOH and $[H_2AsO_3]^-$—FeOOH) are present in the lower portion of the diagram over a wide pH range.

4. Discussion

4.1. Identifying arsenic species in the TMF

The tailings slurry deposited in the TMF consists of a mixture of neutralized raffinate solids and leach residue that may contain primary arsenic minerals. As shown in Fig. 6, the conditions of the TMF are optimized so scorodite is the most stable arsenic species in the TMF. Although the TMF is designed to allow elements to reach a desired mineralogical endpoint, mineralogical evolution is slow. As such,

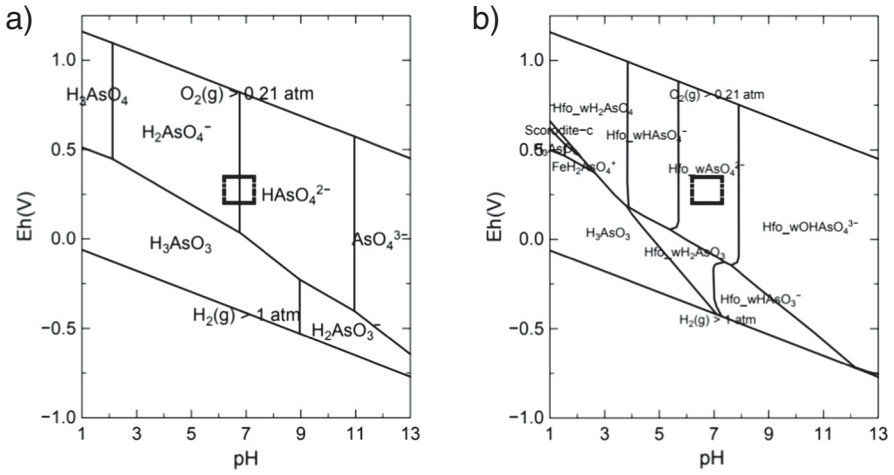

Fig. 8. Eh-pH diagrams for a) the As-O_2-H_2O system at 25 °C showing the soluble arsenic species and b). the As-Fe-Ca-S-O_2-H_2O system where the underlying surface is based upon goethite stability but the surface complexation calculations use the surface complexes described by Gustafsson and Bhattacharya (2007). It is assumed the concentration of geothite is 0.05 mol/L. The Eh and pH range found within the TMF are outlined by the black boxes.

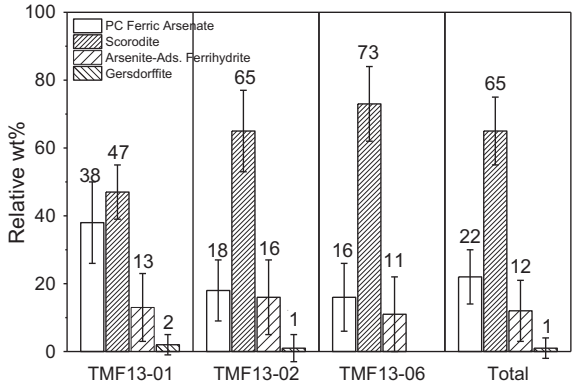

Fig. 9. The distribution of poorly crystalline (PC) iron-containing arsenates, scorodite, arsenite adsorbed on ferrihydrite, and gersdorffite in bore holes TMF13-01, TMF13-02, and TMF13-06. The total distribution of arsenic species is also listed.

multiple arsenic species may be present the TMF. Identifying arsenic-containing species in the TMF is problematic as the tailings samples were found to be composed of mostly quartz, gypsum, and various clay minerals (Hayes et al., 2014). Although there were feature observed in the background of the S-XRD patterns between 5–20° that were consistent with ferrihydrite or poorly crystalline ferric arsenate (See Fig. A8 in the Appendix), arsenic-containing phases could not be conclusively identified from the S-XRD patterns. Diffraction is not an element-specific technique and the presence of other highly crystalline phases can impede detection of minor or poorly crystalline species that may be present in a sample. XANES, however, is an element-specific technique that is capable of detecting crystalline and non-crystalline arsenic species at low concentrations in the tailings samples (i.e. < 100 μg/g). The LCF analysis of the arsenic K-edge XANES spectra indicated that there are multiple arsenic species present in the tailings solids of various oxidation states. In general, arsenic speciation in the TMF can be divided into three groups: arsenate (As^{5+}), arsenite (As^{3+}), and arsenide (As^{1-}) species.

LCF analysis indicated that the tailings samples consist of scorodite and poorly crystalline iron-containing arsenates. Fitting the arsenic K-edge XANES spectra to crystalline scorodite and a poorly crystalline iron-containing arsenate standard accounted for small variations in the intensity of the first peak (see Fig. A62 in the Appendix). Poorly crystalline ferric arsenate or arsenate adsorbed on ferrihydrite could be used as the poorly crystalline iron-containing arsenate standard in the LCF. It was not possible to distinguish between these arsenate species. The As—Fe bond distance and coordination number (i.e. second coordination sphere) in poorly crystalline ferric arsenate and arsenate-adsorbed ferrihydrite are smaller than that observed in crystalline scorodite (Chen et al., 2009), resulting in both poorly crystalline iron-containing arsenates exhibiting similar arsenic K-edge lineshapes. Arsenate adsorbed on ferrihydrite is likely present given the abundance of ferrihydrite in the TMF. Also, as illustrated in Fig. 8b, arsenate adsorbed on ferrihydrite is stable under the conditions of the TMF. Recent studies have shown that amorphous ferric arsenate can form on the surface of arsenate-adsorbed ferrihydrite under near-neutral conditions, slowly crystallizing as poorly crystalline ferric arsenate and ultimately to scorodite (Das et al., 2015; Jia et al., 2007). It is likely that all three arsenate species co-exist in the TMF with scorodite as the only crystalline iron-containing arsenate.

Arsenite adsorbed on ferrihydrite was identified as the only arsenite species in the tailings samples. Surprisingly, arsenite species were not observed in the neutralized raffinate solids (Langmuir et al., 2006; Mahoney et al., 2007; Chen et al., 2009). Given the oxic conditions of the TMF, (see Fig. 6), it is possible that arsenite species form from the oxidation of primary arsenic minerals found within the leach residue component of the tailings slurry deposited in the TMF. The most stable arsenite species under near neutral conditions of the TMF is arsenous acid (see Fig. 8a), which is highly soluble and not expected to precipitate in the TMF (Pokrovski et al., 1996). However, as illustrated in

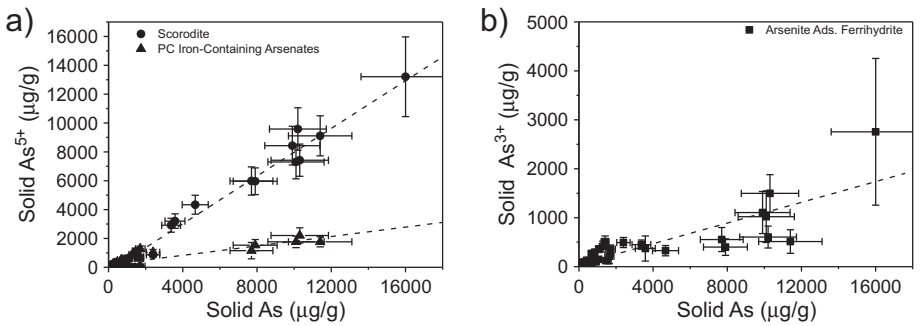

Fig. 10. a) The concentration of scorodite (●) and poorly crystalline (PC) iron-containing arsenates (▲) plotted against the total concentration of arsenic in tailings solids. Note the linear relationships in the concentrations of scorodite (R^2 = 0.976) and poorly crystalline (PC) iron-containing arsenates (R^2 = 0.859) with respect to the total concentration of arsenic in the tailings solids. b) The concentration of arsenite adsorbed on ferrihydrite (■) plotted against the total concentration of arsenic in the tailings solids. Note the linear relationships in the amount of arsenite adsorbed on ferrihydrite (R^2 = 0.737) with respect to the total concentration of arsenic in the tailings solids.

Fig. 7, arsenous acid can adsorb on iron-rich oxides or hydroxides (i.e. ferrihydrite) within the pH range of the TMF. Small amounts of arsenite have been observed to adsorb onto iron-rich clay surfaces in the presence of arsenate (Linz and Puls, 2000). The formation of arsenite adsorbed on ferrihydrite under the conditions of the TMF may be related to both the stability of arsenous acid and the surface charge on the ferrihydrite surface. With increasing pH, the ferrihydrite surface develops a more negative surface charge that repels the more negative surface complexes. If arsenite was to adsorb on ferrihydrite under the near neutral conditions, the dominant surface complex would be a neutral H_3AsO_3–FeOOH surface complex, which is not affected by the negative charge on the ferrihydrite surface. Chemical bonding between the arsenite ion and the ferrihydrite surface will also change with increasing pH. However, it is unlikely to be as pronounced as the changes to electrostatic interactions. The stability field of arsenite adsorbed species are outside the stability field of the TMF (see Fig. 8b), suggesting that arsenite adsorbed species are temporarily in the TMF and will likely undergo further oxidation.

Arsenide species were identified in only six samples at much low concentrations compared to the arsenate and arsenite species. Given the oxic conditions of the TMF (see Fig. 6), arsenides are likely primary minerals that were not fully oxidized during the uranium leaching process and will undergo further oxidation over time. The only two arsenide minerals identified in the tailings samples were gersdorffite and rammelsbergite. Niccolite and skutterudite were not observed in the tailings samples, suggesting that these species were completely oxidized during the leaching and tailings preparation processes.

It should be noted that the majority of arsenic species in the TMF were found to contained iron. However, it would not be possible to confirm arsenic speciation from the iron K-edge XANES. There is significantly more iron in the TMF compared to arsenic (see Table A1 in the Appendix) with most of the iron existing as ferrihydrite. Ferrihydrite acts as a strong adsorber in the TMF, controlling the concentration of various elements such as nickel (Mahoney et al., 2007) and molybdenum (Hayes et al., 2014). Adsorbed ferrihydrite species have very similar Fe K-edge lineshapes since the adsorbed species have little effect on the local structure of iron (Zheng et al., 2014). Given the abundance of ferrihydrite in the TMF, the As K-edge XANES is more suitable for identifying arsenic species.

4.2. Distribution of arsenic species in the TMF

The distribution of the various arsenic species was found to vary across the TMF, as illustrated in Fig. 9. Scorodite is the most abundant species found in the tailings samples, accounting for 65 wt% of the total solid arsenic content in the tailings samples. The concentration of scorodite also increases as the concentration of solid arsenic increases in the TMF, as illustrated in Fig. 10a. This suggests that scorodite is the major arsenic-containing species produced by the tailings preparation process. Higher concentrations of scorodite are found in tailings samples collected from the peripheral bore hole, consistent with finer grains of secondary mineralization drifting towards the periphery of the TMF. The regions of the TMF containing high concentrations of scorodite also corresponded to the lower pH (i.e. slightly < 7) regions of the TMF (see Table A1 in the Appendix), consistent with previous neutralization studies (Chen et al., 2009). As a comparison, relatively larger amounts of poorly crystalline iron-containing arsenates were found in tailings samples collected from the central bore hole (Fig. 9) and showed a smaller correlation with total solid arsenic concentration compared to scorodite (Fig. 10a). Higher concentrations of poorly crystalline iron-containing arsenates near the centre of the TMF may be due to the oxidation of large grains of primary arsenic mineralization followed by the re-precipitation as an oxidized arsenic species.

The relative concentration of arsenite adsorbed on ferrihydrite was fairly consistent across the TMF (see Fig. 9) and also found to increase with the total concentration of solid arsenic (see Fig. 10b). The correlation with total solid arsenic is smaller than that observed with scorodite. Primary arsenide species only accounted for 1 wt% of the total solid arsenic content in the TMF and were identified in samples collected near the centre of the TMF. This is consistent with large grains of primary mineralization collecting in the centre of the TMF. Note that the amount of primary arsenide species in the TMF is significantly lower than that remains after acid leaching the source ore (~5–30 wt%). This indicates that primary arsenides undergo further oxidation downstream of the acid leaching process at the MLO.

5. Conclusions

Arsenic K-edge XANES was determined to be the optimum technique for identifying arsenic species in the TMF due to the abundance of other crystalline phases and the poorly crystalline nature of arsenic species. Arsenic K-edge XANES analysis concluded that scorodite was the most abundant arsenic species in the tailings samples, with high concentrations found in the periphery of the TMF. The high concentrations of scorodite suggest that most of the arsenic in the TMF originates as a chemical precipitate in the neutralized raffinate solid component of the tailings slurry. Relatively larger amounts of poorly crystalline iron-containing arsenates were found in tailings samples collected from the centre of the TMF, suggesting that it may form from the oxidation and reprecipitation of primary arsenic mineral species. The remaining arsenic species found in the TMF were arsenite species in the form of arsenite adsorbed on ferrihydrite and primary arsenides in the form of gersdorffite and rammelsbergite. The small amount arsenides in the ore suggests that the majority of the original primary arsenic minerals in the leached residue was oxidized downstream of the acid leaching process at the MLO. Thermodynamic calculations indicated that arsenite adsorbed on ferrihydrite is not stable under the conditions of the TMF and will undergo further oxidation. Overall, the results are consistent with the studies performed in support of the MLO that predicted arsenic in the tailings will exist primarily as scorodite. The strong correlation between the concentration of scorodite and total concentration of solid arsenic in the tailings also confirms the processes used at the MLO to prepare the tailings for long term storage can respond to wide range of arsenic concentrations found in uranium-containing ores.

Acknowledgments

The authors would like to extend their thanks to Dr. Ning Chen and Dr. Weifeng Chen for their help performing measurements on the HXMA beamline (06-ID1; CLS). The authors would also like to thank members of the Industrial Science group (Erika Bergen, Toby Bond, Jeremy Olson) for their technical assistance. The CLS is funded by the Canadian Foundation of Innovation (CFI), the National Science and Engineering Research Council (NSERC), The National Research Council (NRC), the Canadian Institutes of Health Research (CIHR), the Government of Saskatchewan, and the University of Saskatchewan. The Cameco Corporation and the Royal Ontario Museum are thanked for providing mineral standards.

Appendix A. Supplementary data

Supplementary data to this article can be found online at http://dx.doi.org/10.1016/j.chemgeo.2017.07.014.

References

AREVA Resources Canada Ltd. (AREVA), 2015. McClean Lake operation technical information document (TID): tailings management. Version 02. Revision 00. Section 5.6: verification of long-term tailings geochemistry. 5-110–5-123. A copy of the report can be requested from AREVA Resources Canada (e-mail: publicrelations@areva.ca) or the Canadian Nuclear Safety Commission. http://nuclearsafety.gc.ca/eng/uranium/mines-and-mills/nuclear-facilities/mcclean-lake/index.cfm.

Beauchemin, S., Hesterberg, D., Beauchemin, M., 2002. Principal component analysis approach for modeling sulfur K-XANES spectra of humic acids. Soil Sci. Soc. Am. J. 66, 83–91.
Chen, N., Jiang, D.T., Cutler, J., Kotzer, T., Jia, Y.F., Demopoulos, G.P., Rowson, J.W., 2009. Structural characterization of poorly-crystalline scorodite, iron(III)-arsenate co-precipitates and uranium mill neutralized raffinate solids using X-ray absorption fine structure spectroscopy. Geochim. Cosmochim. Acta 73, 3260–3276.
Das, S., Essilfie-Dughan, J., Hendry, J.M., 2015. Fate of adsorbed arsenate during phase transformation of ferrihydrite in the presence of gypsum and alkaline conditions. Chem. Geol. 411, 69–80.
Dzombak, D.A., Morel, F.M.M., 1990. Surface Complexation Modeling - Hydrous Ferric Oxide. John Wiley and Sons, New York.
Essilfie-Dughan, J., Hendry, M.J., Warner, J., Kotzer, T., 2013. Arsenic and iron speciation in uranium mine tailings using X-ray absorption spectroscopy. Appl. Geochem. 28, 11–18.
Fernández-García, M., Márquez Alvarez, C., Haller, G.L., 1995. XANES-TPR study of Cu-Pd bimetallic catalysts: applications of factor analysis. J. Phys. Chem. 99, 12565–12569.
Fodje, M., Grochulski, P., Janzen, K., Labiuk, S., Gorin, J., Berg, R., 2014. 08B1-1: an automated beamline for macromolecular crystallography experiments at the Canadian Light Source. J. Synchrotron Radiat. 21, 633–637.
Foster, A.L., Kim, C.S., 2014. Arsenic speciation in solids usings X-ray absorption spectroscopy. Rev. Mineral. Geochem. 79, 257–369.
Foster, A.L., Brown Jr., G.E., Tingle, T.N., Parks, G.A., 1998. Quantitative arsenic speciation in mine tailings using X-ray absorption spectroscopy. Am. Mineral. 83, 553–568.
Gustafsson, J.P., Bhattacharya, P., 2007. Geochemical modeling of arsenic adsorption to oxide surfaces. (Chapter 6). In: Bhattacharya, P., Mukherjee, A.B., Bundschuh, J., Zevenhoven, R., Loeppert, R.H. (Eds.), Arsenic in Soil and Groundwater Environment. Trace Metals and Other Contaminants in the Environment, vol. 9. Elsevier B.V., pp. 159–206.
Hayes, J.R., Grosvenor, A.P., Rowson, J., Hughes, K., Frey, R.A., Reid, J., 2014. Analysis of the Mo speciation in the JEB Tailings Management Facility at McClean Lake, Saskatchewan. Environ. Sci. Technol. 48, 4460–4467.
Hoeve, J., Quirt, D.H., 1987. A stationary redox front as a critical factor in the formation of high grade unconformity-type uranium ores in the Athabasca basin, Saskatchewan, Canada. Bull. Mineral. 110, 157–171.
Jia, Y., Xu, L., Wang, X., Demopoulos, G.P., 2007. Infrared spectroscopic and X-ray diffraction characterization of the nature of adsorbed arsenate on ferrihydrite. Geochim. Cosmochim. Acta 71, 1643–1654.
Jiang, D.T., Chen, N., Zhang, L., Malgorzata, G., Wright, G., Igarashi, R., Beauregard, D., Kirkham, M., McKibben, M., 2007. XAFS at the Canadian Light Source. AIP Conf. Proc. 882, 893–895.
Kinniburgh, D.G., Cooper, D.M., 2011. PhreePlot – creating graphical output with PHREEQC. Available at. http://www.phreeplot.org/.
Kutzler, F.W., Natoli, C.R., Misemer, D.K., Donjach, S., Hodgson, K.O., 1980. Use of one electron theory for the interpretation of near edge structure in K-shell X-ray absorption spectra of transition metal complexes. J. Chem. Phys. 73, 3274–3288.
Langmuir, D., Mahoney, J.J., MacDonald, A.K., Rowson, J., 1999a. Predicting the arsenic source-term from buried uranium mill tailings. In: Proc. Tailings and Mine Waste '99. Fort Collins, Colorado, pp. 503–514.
Langmuir, D., Mahoney, J., MacDonald, A., Rowson, J., 1999b. Predicting arsenic concentrations in the porewaters of buried uranium mill tailings. Geochim. Cosmochim. Acta 63, 3379–3394.
Langmuir, D., Mahoney, J., Rowson, J., 2006. Solubility products of amorphous ferric arsenate and crystalline scorodite ($FeAsO_4{\cdot}2H_2O$) and their application to arsenic behavior in buried mine tailings. Geochim. Cosmochim. Acta 70, 2942–2956.
Lin, J., Chen, N., Pan, Y., 2014. Arsenic speciation in newberyite ($MgHPO_4{\cdot}3H_2O$) determined by synchrotron X-ray absorption and electron paramagnetic resonance spectroscopies: implications for the fate of arsenic in green fertilizers. Environ. Sci. Technol. 48, 6938–6946.
Linz, Z., Puls, R.W., 2000. Adsorption, desorption and oxidation of arsenic affected by clay minerals and aging process. Environ. Geol. 39, 753–759.
Mahoney, J., Slaughter, M., Langmuir, D., Rowson, J., 2007. Control of As and Ni releases from a uranium mill tailings neutralization circuit: solution chemistry, mineralogy and geochemical modelling of laboratory study results. Appl. Geochem. 22, 2758–2776.
Malinowski, E.R., 2002. Factor Analysis in Chemistry, 3rd ed. John Wiley & Sons, New York.
Moldovan, B.J., Hendry, M.J., 2005. Characterizing and quantifying controls on arsenic solubility over a pH range of 1–11 in a uranium mill-scale experiment. Environ. Sci. Technol. 39, 4913–4920.
Moldovan, B.J., Jiang, D.T., Hendry, M.J., 2003. Mineralogical characterization of arsenic in uranium mine tailings precipitated from iron-rich hydrometallurgical solutions. Environ. Sci. Technol. 37, 873–879.
Newville, M., 2004. Fundamentals in XAFS. Consortium for Advanced Radiation Sources. University of Chicago, Chicago.
Paktunc, A.D., Szymanski, J., Lastra, R., Laflamme, J.H.G., Enns, V., Soprovich, E., 1998. Assessment of potential arsenic mobilization from the Ketza River mine tailings, Yukon, Canada. In: Petruk, W. (Ed.), Waste Characterization and Treatment. Soc. Mining Metallurgy & Exploration, Inc., pp. 49–60.
Paktunc, D., Foster, A., Laflamme, G., 2003. Speciation and characterization of arsenic in Ketza River Mine Tailings using X-ray absorption spectroscopy. Environ. Sci. Technol. 37, 2067–2074.
Paktunc, D., Foster, A., Heald, S., Laflamme, G., 2004. Speciation and characterization of arsenic in gold ores and cyanidation tailings using X-ray absorption spectroscopy. Geochim. Cosmochim. Acta 68, 969–983.
Parkhurst, D.L., Appelo, C.A.J., 2013. Description of input and examples for PHREEQC version 3 — a computer program for speciation, batch-reaction, one-dimensional transport, and inverse geochemical calculations: U.S. Geological Survey Techniques and Methods, book 6. available only at. http://pubs.usgs.gov/tm/06/a43.
Pichler, T., Hendry, M.J., Hall, G.E.M., 2001. The mineralogy of arsenic in uranium mine tailings at the Rabbit Lake in-pit facility, northern Saskatchewan, Canada. Environ. Geol. 40, 495–506.
Pokrovski, G., Gout, R., Schott, J., Zotov, A., Harrichoury, J.C., 1996. Thermodynamic properties and stoichiometry of As(III) hydroxide complexes at hydrothermal conditions. Geochim. Cosmochim. Acta 60, 737–749.
Powder Diffraction File, 2013. Web-PDF-4 +. In: International Centre for Diffraction Data, Newtown Square, Pennsylvania, USA.
Ravel, B., Newville, M., 2005. ATHENA, ARTEMIS, HEPHAESTUS: data analysis for X-ray absorption spectroscopy using IFEFFIT. J. Synchrotron Radiat. 12, 537–541.
Rehr, J.J., Albers, R.C., 2000. Theoretical approaches to X-ray absorption fine structure. Rev. Mod. Phys. 72, 621–654.
Reyx, J., Ruhjmann, F., 1993. Metallurgical study of different mineral associations and chemical characterization of the deposit of uranium minerals in Cigar Lake (Saskatchewan, Canada). Can. J. Earth Sci. 30, 705–719.
Robertson, J., Shacklock, K., Frey, R., Gomez, M.A., Essilfie-Dugan, J., Hendry, M.J., 2014. Modelling the Key Lake uranium mill's bulk neutralization process using a pilot-scale model. Hydrometallurgy 149, 220–227.
Roussel, C., Neel, C., Bril, H., 2000. Minerals controlling arsenic and lead solubility in an abandoned gold mine tailings. Sci. Total Environ. 263, 209–219.
Shaw, S., Hendry, J.M., Essilfie-Dughan, J., Kotzer, T., Wallschlager, D., 2011. Distribution, characterization, and geochemical controls of elements of concern in uranium mine tailings, Key Lake, Saskatchewan, Canada. Appl. Geochem. 26, 2044–2056.
Toby, B.H., Von Dreele, R.B., 2013. GSAS II: the genesis of a modern open-source all purpose crystallography software package. J. Appl. Crystallogr. 46, 544–549.
Wang, Y., Jiao, J.J., Zhu, S., Li, Y., 2013. Arsenic K-edge X-ray absorption near-edge spectroscopy to determine oxidation states of arsenic of a coastal aquifer-aquitard system. Environ. Pollut. 179, 160–166.
Zheng, G., Liu, F., Liu, H., Qu, J., Liu, R., 2014. Respective role of Fe and Mn oxide contents for arsenic sorption in iron and manganese binary oxide: an X-ray absorption spectroscopy investigation. Environ. Sci. Technol. 48, 10316–10322.